Modeling fluid-solid thermomechanical interactions in casting processes

Marcela A. Cruchaga and Diego J. Celentano
Departamento de Ingeniería Mecánica, Universidad de Santiago Chile, Santiago, Chile

Roland W. Lewis
School of Engineering, University of Wales, Swansea, UK

Received December 2002
Revised January 2003
Accepted January 2003

Keywords *Fluid dynamics, Metals, Metallurgy*

Abstract *An integrated formulation for the analysis of casting processes is presented in this work. This model involves the description of the evolution and the coupled interactions of the flow, thermal and mechanical fields occurring during the liquid-solid transformation of the solidifying metal. The corresponding discretized formulation is solved in the context of a fixed-mesh finite element method. Numerical results applying this methodology in two cylindrical casting specimens are first presented to assess the influence of different phenomena occurring during the process. Moreover, these simulations are compared with available experimental data.*

1. Introduction

It is a very well-known fact that metal casting processes are complex problems that combine different physical phenomena such as fluid flow (mould filling and natural convection), heat transfer, phase-change evolution and thermal residual stress development. The different phenomena involved in casting processes can be described within the context of several interdependent fields. Figure 1 schematically shows a classical decomposition for the analysis of solidification problems. The fluid (F), thermal (T), mechanical (M) and microstructural (S) fields may be, respectively, characterized by the following state variables ($\mathbf{v}$, p), (T, $\dot{T}$), ($\mathbf{u}$, g_n, $\boldsymbol{\sigma}$) and (f_{pc}, R), where $\mathbf{v}$ is the velocity vector, p the pressure, T the temperature, the superposed dot denotes time partial derivative, $\mathbf{u}$ is the displacement vector, g_n is the normal gap that develops at the casting-mould interface, $\boldsymbol{\sigma}$ is the stress tensor, f_{pc} is the phase-change function (liquid fraction) describing the material transformations and R symbolically indicates any microstructural variable of interest (such as the grain radius). As can be seen, these fields are strongly coupled by means of six two-directional interactions which take into account, for instance, the

The supports provided by the Chilean Council for Research and Technology CONICYT (FONDECYT Project No. 1020029-7020029) and the Department of Technological and Scientific Research at the Universidad de Santiago de Chile are gratefully acknowledged.

International Journal of Numerical Methods for Heat & Fluid Flow
Vol. 14 No. 2, 2004
pp. 167-186

0961-5539
DOI 10.1108/09615530410513791

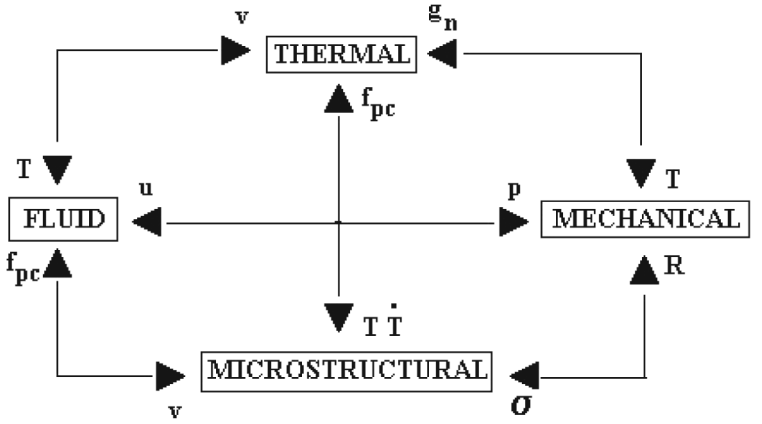

Figure 1.
Interdependent fields for the analysis of solidification problems

thermally-driven fluid motion (FT), changes in the energy balance and in the material properties due to microstructural phase-change (FS, TS and MS), the presence of advective effects in the energy equation and in the microstructural evolution laws (FT and FS), the reduction in the heat transfer conditions at the casting-mould interface owing to gap formation (TM), the development of thermal strains and stresses in the solid (TM), the motion and forces that take place at the liquid-solid interface (FM) and finally, the influence of stresses on the microstructure evolution (MS). In general, these interactions have received much attention in the casting literature. In particular, thermally coupled fluid dynamics analyses considering a macroscopic (i.e. only temperature-dependent) phase-change approach (FT) have been reported for the evaluation of natural convection occurring during solidification (Cruchaga and Celentano, 2000, 2001; Guthrie and Tavares, 1998; Nigro *et al.*, 2000; Yun *et al.*, 2000 and references therein) within the framework of different numerical methods and latent heat release models. In addition, filling simulations with and without phase-change effects have been performed by means of front-capturing or front-tracking techniques (Cruchaga and Celentano, 2002; Cruchaga *et al.*, 2002a; Lewis and Ravindran, 2000). Most of these models have been extended to account for microstructural formation during phase-change (FTS) defining, to this end, either kinetic-based laws for the evolution of the transformed phases (Celentano and Cruchaga, 1999; Sobh *et al.*, 2000) or species conservation (Heinrich and McBride, 2000; Naterer, 1997) including freckle development (Felicelli *et al.*, 1998), macrosegregation (Gu and Beckermann, 1999; Vreeman and Incropera, 2000; Vreeman *et al.*, 2000), microsegregation (Voller, 2000; Voller and Beckermann, 1999) and hot-tearing prediction (Rappaz *et al.*, 1999). On the other hand, different thermomechanical formulations (TM) have been proposed to describe the casting and mould material responses during the solidification and cooling stages (Bellet *et al.*, 1996; Celentano *et al.*, 1999). Such description usually encompasses variable

thermomechanical contact conditions caused by gap formation that takes place at the casting-mould interface, plastic or viscoplastic effects with temperature-dependent material properties and the consideration of phase-change strains in the constitutive laws. In this last context, models of microstructure evolution (TMS) have been included to represent some physical aspects involved in the process in a more realistic form (Celentano, 2001, 2002). Moreover, finite-volume numerical simulations including fluid-thermomechanical interactions (FTM) have been presented by Chow *et al.* (1995). Although all the above mentioned models have been successfully exploited during the last years, a fully integrated formulation able to properly predict the physically relevant interactions existing in the complete casting process can be considered nowadays as a challenging subject of research.

In this work, a coupled multi-physics model for the analysis of solidification processes is presented. This model is targeted at the material description of the liquid, mushy and solid phases occurring during the filling, solidification and subsequent cooling of the casting. In particular, the aim of this paper is to assess the fluid motion influence on the temperature and casting-mould gap evolutions when advective effects in the liquid phase are considered. To this end, buoyancy forces as well as phase-change effects are considered during both the filling and solidification stages. Other motivation of this study is the evaluation of non-uniform initial temperature pattern in the solidification and cooling stages. This situation, obtained as a result of the filling, is in contrast to the uniform initial distribution extensively assumed in the modeling of this process. The consideration of buoyancy effects and phase-change during the whole process couples the fluid phase motion with the thermal and mechanical responses through the fluid velocity, temperature field and the gap formation.

The proposed multi-physics model accounting for fluid-solid thermomechanical interactions in castings is presented in Section 2. Section 3 briefly describes the main features of the corresponding discretized formulation defined in the finite element context. The performance of this methodology is checked, in Section 4, in the analysis of two solidification tests by assessing the influence of different physical aspects on the material response. In addition, numerical results obtained with this methodology are compared with experimental measured data.

2. Integrated model

In this work, the analysis of casting processes is split into three different coupled stages: mould filling, solidification and cooling. The filling of a mould cavity initially occupied by air is described through a thermally coupled incompressible flow formulation considering either Newtonian or turbulent behavior for both the molten metal and air. Both phase-change and buoyancy effects are considered during the filling. Owing to the rapid evolution of the filling process, no significant mould motion is assumed at this stage.

The solidification stage involves natural convection in the liquid as well as in the mushy zone, a macroscopic phenomenological (only temperature-dependent) constitutive law for the solid fraction evolution and, moreover, a description of the thermomechanical response in the casting and mould materials. These thermomechanical aspects are considered by a large strain thermoviscoplastic constitutive model. Variable thermomechanical contact conditions caused by gap development at the casting-mould interface are also considered. Finally, the third stage takes place once the liquid-solid phase-change is completely finished until the final cooling to room temperature.

In this context, the mushy behavior is described using the flow equations. Nevertheless, more complex models in the description of this zone may be needed. It is also important to remark that the thermally coupled flow responses for the liquid and mushy phases are computed assuming small displacements at the liquid-solid and mushy-solid boundaries, i.e. a negligible difference between material and spatial coordinates in such regions is considered.

In the thermally coupled flow and thermomechanical formulations involved in this proposed model, the domain of the analysis Ω can be split as $\Omega = \Omega_{\mathrm{l}} \cup \Omega_{\mathrm{m}} \cup \Omega_{\mathrm{s}}$ where subscripts l, m and s denote liquid, mushy and solid phases, respectively. The liquid domain can be decomposed, in turn, as $\Omega_{\mathrm{l}} = \Omega_{\mathrm{lc}} \cup \Omega_{\mathrm{la}}$ such that Ω_{lc} and Ω_{la} are the domains occupied by the molten metal and air, respectively. It should be noted that all these regions are time-varying domains. All the equations of the model are solved in the time interval of interest $Y (t \in Y)$. Details of such formulations are separately described below.

2.1 Thermally coupled flow formulation

The thermally coupled Navier-Stokes equations of unsteady incompressible flows can be used to describe the natural and forced convections in the liquid phase for melting and solidification processes. These equations (Eulerian description) consist of the momentum equation, the incompressibility constraint and the heat transfer balance written as follows (Cruchaga and Celentano, 2001):

$$\rho \dot{\mathbf{v}} + \rho(\mathbf{v} \cdot \nabla)\mathbf{v} + \nabla p - \nabla \cdot (2\mu \boldsymbol{\varepsilon}) = \rho \mathbf{b} \quad \text{in } \Omega_{\mathrm{l}} \cup \Omega_{\mathrm{m}} \times Y \tag{1}$$

$$\nabla \cdot \mathbf{v} = 0 \quad \text{in } \Omega_{\mathrm{l}} \cup \Omega_{\mathrm{m}} \times Y \tag{2}$$

$$\rho c\left(\dot{T} + \mathbf{v} \cdot \nabla T\right) + \rho L\left(\dot{f}_{\mathrm{pc}} + \mathbf{v} \cdot \nabla f_{\mathrm{pc}}\right) = \nabla \cdot (k \nabla T) + \rho r + 2\mu \boldsymbol{\varepsilon} : \boldsymbol{\varepsilon} \quad \text{in } \Omega_{\mathrm{l}} \cup \Omega_{\mathrm{m}} \times Y \tag{3}$$

together with appropriate boundary and initial conditions. In these equations, standard notation is used: ρ is the density, μ is the dynamic viscosity, $\mathbf{v}$ is the

velocity vector, p is the pressure, $\mathbf{b}$ is the specific body force vector, $\boldsymbol{\varepsilon}$ is the rate-of-deformation tensor ($\boldsymbol{\varepsilon} = 1/2(\nabla \times \mathbf{v} + \mathbf{v} \times \nabla)$), T is the temperature, c is the heat capacity, L is the specific latent heat, k is the isotropic conductivity coefficient, r is the specific heat source and $f_{\mathrm{pc}} = f_{\mathrm{pc}}(T)$ is the phase-change function. The symbol ∇ denotes the spatial gradient operator and the dot over a variable represents its time derivative. In order to consider the buoyancy effects, the specific body force vector is written according to the Boussinesq approximation as $\mathbf{b} = \mathbf{g}[1 - \alpha(T - T_{\mathrm{ref}})]$, where $\mathbf{g}$ is the gravity vector α is the volumetric thermal dilatation coefficient and T_{ref} is a reference temperature value.

This formulation is applied to the liquid and mushy phases during the solidification stage. Assuming an equiaxed morphology development during phase-change, the dynamic viscosity in the mushy region can be given by $\mu = \mu_{\mathrm{l}}/f_{\mathrm{pc}}$ (Celentano and Cruchaga, 1999).

To describe the filling process, an additional equation accounting for the casting-air interface motion has to be considered (Tezduyar, 2001):

$$\dot{\varphi} + \mathbf{v} \cdot \nabla \varphi = 0 \quad \text{in } \Omega_{\mathrm{l}} \times Y \tag{4}$$

where φ is a marker function to identify the materials involved (e.g. $\varphi = 1$ for the casting and $\varphi = 0$ for the air). In this context, a generic material property P is obtained as $P = \varphi P_{\mathrm{lc}} + (l - \varphi) P_{\mathrm{la}}$. Moreover, a simple mixed length based turbulent model was used to simulate both fluid behavior (metal and air) at this stage, i.e. $\mu = \mu_l + \rho_{\mathrm{l}} l_{\mathrm{mix}}^2 \gamma$, where l_{mix} is the mixing length that is taken here as the vortex length and γ is the effective strain rate $\sqrt{2/3\boldsymbol{\varepsilon} : \boldsymbol{\varepsilon}}$.

2.2 Thermomechanical formulation

A general thermomechanical process can be described by the following form of the governing local equations (Lagrangian description) expressed by the mass conservation, the equation of motion, the energy balance and the dissipation inequality (Celentano, 2001, 2002):

$$\rho J = \rho_0 \quad \text{in } \Omega_{\mathrm{s}} \times Y \tag{5}$$

$$\nabla \cdot \boldsymbol{\sigma} + \rho \mathbf{b}_{\mathrm{f}} = \rho \ddot{\mathbf{u}} \quad \text{in } \Omega_{\mathrm{s}} \times Y \tag{6}$$

$$\rho c \dot{T} + \rho L \dot{f}_{\mathrm{pc}} = \nabla \cdot (k \nabla T) + \rho r - T \boldsymbol{\beta} : \boldsymbol{\varepsilon} + \rho r_{\mathrm{int}} \quad \text{in } \Omega_{\mathrm{s}} \times Y \tag{7}$$

$$k \nabla T \cdot \nabla T + D_{\mathrm{int}} \geq 0 \quad \text{in } \Omega_{\mathrm{s}} \times Y \tag{8}$$

together with appropriate boundary and initial conditions and the constitutive relations assumed to be given by classical expressions depending on the specific Helmholtz free energy function $\psi = \psi(\mathbf{e}, \alpha_k, T) : \boldsymbol{\sigma} = \rho \, \partial \psi / \partial \mathbf{e}$ is the

Cauchy stress tensor, $\eta = -\partial\psi/\partial T$ is the specific entropy function, $c = -T\,\partial^2\psi/\partial T^2$ is the tangent specific heat capacity, $\beta = -\rho\,\partial^2\psi/\partial\mathbf{e}\partial T = -\partial\boldsymbol{\sigma}/\partial T$ is the tangent conjugate of the thermal dilatation tensor,

$$r_{\text{int}} = -1/\rho\left(T\frac{\partial\mathbf{q}_k}{\partial T} - \mathbf{q}_k\right) * \frac{\mathrm{D}\alpha_k}{\mathrm{D}t}$$

is the specific internal heat source and

$$D_{\text{int}} = \mathbf{q}_k * \frac{\mathrm{D}\alpha_k}{\mathrm{D}t}$$

is the internal dissipation where $\mathbf{e}$ is the Almansi strain tensor, α_k is a set of phenomenological internal state variables usually governed by evolution laws and $\mathbf{q}_k = -\rho\partial\psi/\partial\alpha_k$ are the conjugate variables of α_k. According to the nature of each internal variable, the symbols * and $\mathrm{D}(\cdot)/\mathrm{D}t$ appearing in the previous expressions, respectively, indicate an appropriate multiplication and a time derivative satisfying the principle of material frame-indifference. Moreover, ρ is the density at the spatial configuration, ρ_0 is the density at the material (initial) configuration, $\mathbf{b}_{\text{f}}$ is the specific body force, $\mathbf{u}$ is the displacement vector, $J > 0$ is the determinant of the deformation gradient tensor $\mathbf{F}(\mathbf{F}^{-1} = \mathbf{1} - \nabla\times\mathbf{u}$, with $\mathbf{1}$ being the unity tensor) and $v = \dot{\mathbf{u}}$. Instead of equation (8), an additional more restrictive dissipative assumption reads: $k\nabla T\cdot\nabla T \geq 0$ and $D_{\text{int}} \geq 0$. The first condition is automatically fulfilled for a non-negative conductivity coefficient while the second imposes restrictions over the constitutive model definition.

It should be noted that the definition of ψ is a crucial aspect of the formulation since it describes the coupled thermomechanical behavior of all the materials involved in the solidification process. To this end, it is first necessary to establish the expressions of $\mathrm{D}\alpha_k/\mathrm{D}t$ defined in this work within the thermoviscoplasticity context. Further details of this formulation can be found in the work of Celentano (2001, 2002).

3. Finite element model

In the context of the finite element method, the weak form of the equations (1)-(3) can be obtained using a generalized streamline operator technique (Cruchaga and Celentano, 2001). This technique enables the use of equal order interpolation function for the primitive variables of the problem (velocity, pressure and temperature) and involves stabilization terms for the convective, pressure gradient and incompressibility constraint. Moreover, the phase-change effects are treated through a temperature-based fixed-mesh algorithm able to deal with either isothermal or non-isothermal phase-changes. The time integration is carried out with the Euler-backward scheme.

On the other hand, the motion of the interface between two immiscible fluids is updated via an improved fixed-mesh algorithm called edge-tracked interface

locator technique (ETILT). According to ETILT, the current front is determined by solving equation (4) applied in this case to a function φ which is a volume preserving projected function of the interface such that this interface still remains being represented by a Heaviside function. This methodology has been designed by considering the ease in managing a node-based interface representation, interface sharpness and volume conservation features of the moving Lagrangian interface technique (Cruchaga *et al.*, 2002a). The ETILT was originally presented by Tezduyar (2001) and its computational implementation was proposed by Cruchaga *et al.* (2002b).

The weak form of equations (5)-(7) is also derived in the context of the finite element method. Assuming standard spatial interpolations for the displacement and temperature fields, the integration of the terms containing time derivatives of $\mathbf{u}$ and T is, respectively, performed with the Newmark method and the generalized mid-point rule choosing the appropriate parameters that make both algorithms unconditionally stable. The latter scheme has also been used to integrate all the internal rate equations involved in the constitutive thermoviscoplastic model. It is important to remark that a gap-dependent heat transfer coefficient at the casting-mould interface is considered since the strong diminution observed in it, once the gap is formed, can be extremely important in many casting situations. Moreover, a methodology to overcome the volumetric locking effect when incompressible viscoplastic flows takes place is an additional important feature involved in the numerical solution of this thermomechanical model (for further details, see Celentano (2001, 2002).

The integrated model is solved via a staggered scheme that couples the fluid, thermal and mechanical fields through the following interactions (Figure 1): FT ($\mathbf{v}$, T and f_{pc}), FM (only p) and TM (T, f_{pc} and g_{n}).

4. Simulations and experimental validations

4.1 Aluminum alloy solidification test

The performance of the proposed methodology is preliminarily tested in an aluminum alloy casting problem. This proposed simple test is commonly used in the industry to quickly evaluate a range of admissible casting composition indirectly obtained by temperature measurements. The molten metal is poured into a cylindrical cavity mould (height = 62 mm and diameter = 50 mm) as shown in Figure 2. In the present work, the influence of the advective effects induced by filling and buoyancy forces on the casting material response is particularly studied. Moreover, the results obtained using two mould materials with different thermal diffusivities are analyzed with the aim of assessing the effect of the cooling rate on the temperature evolution. Several Al-7 Si alloy casting experiments were carried out at different pouring temperatures in sand and steel moulds to obtain part and mould temperature measurements at the midheight of the specimen (thermocouples 1 and 2, respectively; see Figure 3).

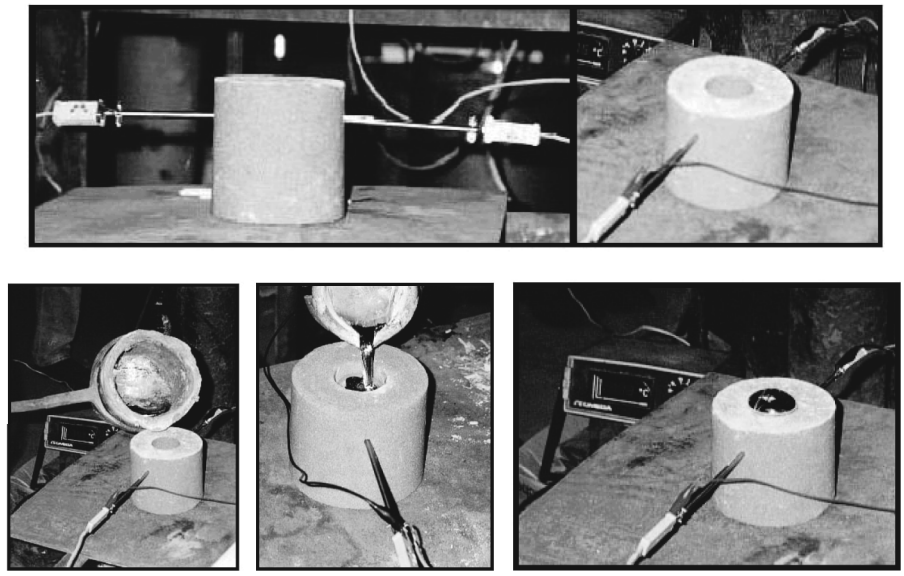

Figure 2.
Aluminum alloy solidification test. Experimental setup and filling sequence

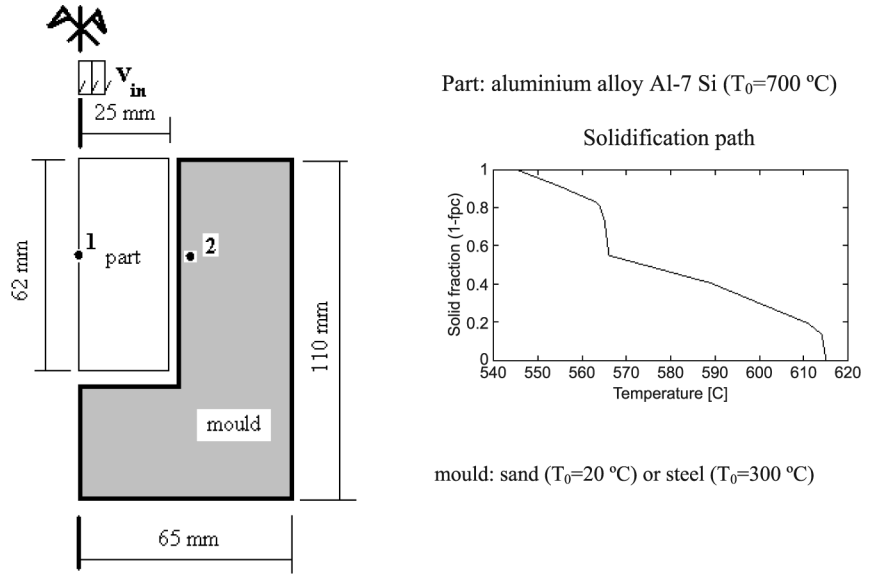

Figure 3.
Aluminum alloy solidification test. (a) Problem layout and (b) material description

Average temperature evolutions based on a set of measurements obtained with enough repeatability are used to compare the numerical results. The aluminum phase-change is macroscopically described through a phenomenological solid-fraction temperature-dependent law also described in Figure 3. The main assumption in the use of such curve is the consideration of a unique

solidification path in the whole casting. This approximation is valid only when approximately uniform cooling rates take place.

In the numerical analysis, the Al-7 Si alloy is poured into the mould at 700°C. The thermophysical properties related to the materials (aluminum alloy, sand and steel) and interfaces (casting-mould, casting-air and mould-air) involved in the process can be found in the work of Celentano (2001), Celentano *et al.* (1999) and Cruchaga and Celentano (2000, 2001). In particular, it should be noted that a gap-dependent heat transfer coefficient is adopted for the casting-mould interface (Celentano *et al.*, 1999). The mixing length for the turbulent model used during filling has been chosen as 10 mm. The finite element mesh consisted of 5,000 and 4,900 four-noded axisymmetric isoparametric elements for the casting and mould, respectively. The time step used in the filling process is 0.001 s while 0.5 s has been considered for both the solidification and cooling stages. An inflow velocity of $v_{in}=0.5$ m/s with a jet radius of 6.5 mm (estimated values in accordance with the flow rate achieved in the experiments) has been imposed at the top boundary. The filling is stopped at 1.8 s (time interval related to the end of the pouring in the experiments).

4.1.1 Casting in a sand mould. In this casing test, the alloy is poured into a resin sand mould initially at 20°C. Figure 4(a) shows the computed material front position at different instants of the filling. Moreover, a simple physical filling experience has been performed using coloured water. A set of photographs is shown in Figure 4(b). From the comparison between the physical and numerical results the following comments can be done. The numerical model does not capture the impingement on the bottom at the initial instants. Nevertheless, after this impact the molten material flows up close to the lateral walls reaching a more ordered regime up to the end of the filling. In such instants the free surface evolves almost horizontally. These facts are also found in the numerical simulation. One of the features of the interface capturing technique used to describe the moving front position is the volume preserving algorithm involved in the methodology which guarantees a correct description of the volume evolution during filling and, consequently, a proper computation of the final filling time. After the stop of the filling (1.8 s), a short simulation of the interface stabilization (horizontal equilibrium position) is performed up to 2.0 s (Figure 4(a)).

To evaluate the influence of buoyancy driven forces during filling on the thermal and fluid patterns, two analyses (with and without buoyancy effects) are performed. Figure 5 summarizes the obtained results. The streamlines and temperatures denote that buoyancy effects do not play a significant role in the molten metal while they only slightly modify the air behavior in such a way to promote a more uniform temperature field in this medium.

In the following analyses, the filling, solidification and cooling stages are modeled in a unified fluid-thermomechanical (FTM) simulation that also includes both buoyancy and phase-change effects. Moreover, a gap-dependent

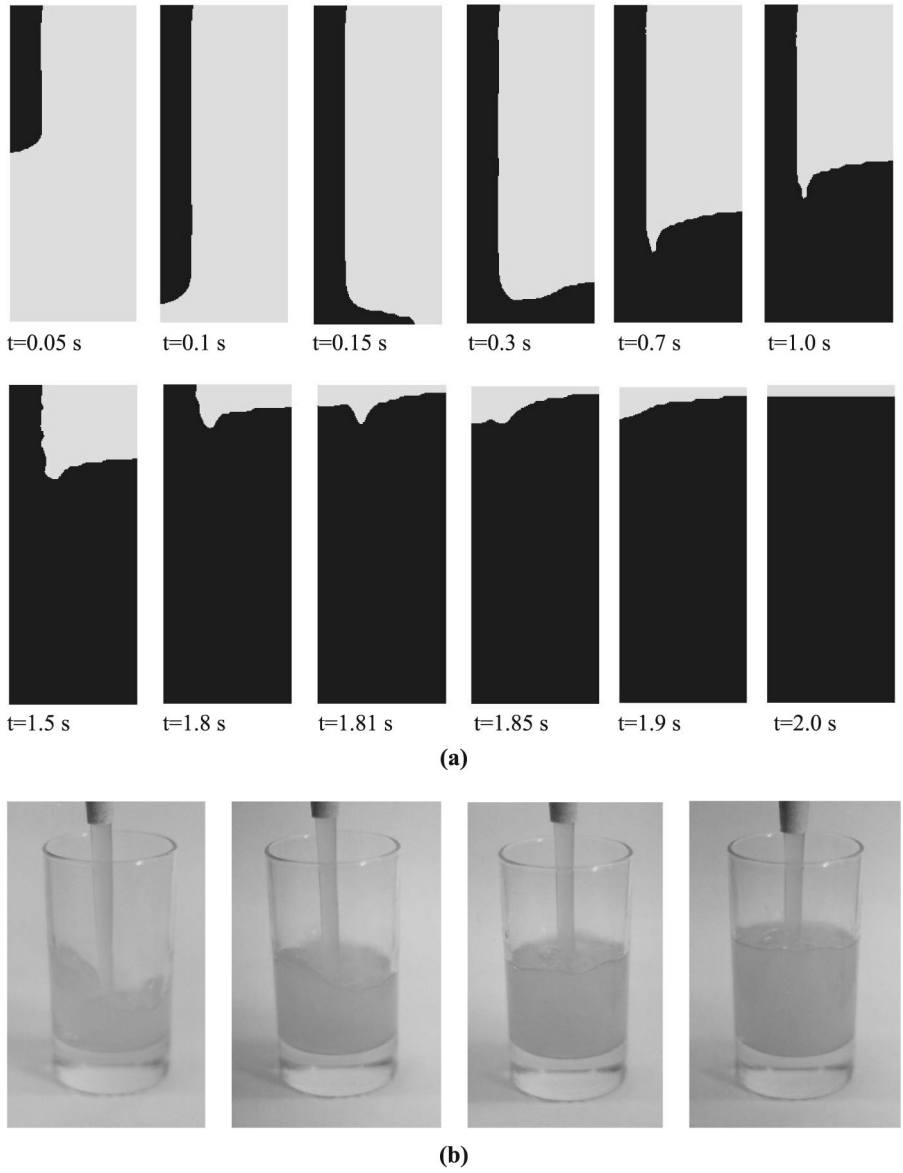

Figure 4.
Aluminum alloy solidification test in a sand mould. (a) Different instants of the filling stage, and (b) simple experimental test with coloured water

heat transfer coefficient is used to consider a more realistic description of the heat flow at the casting-mould contact interface.

The phase-change function sequence during filling is plotted in Figure 6. These results show that the molten metal remains practically liquid in this stage of the processes. A small mushy zone at the tip of the metal jet is obtained at early

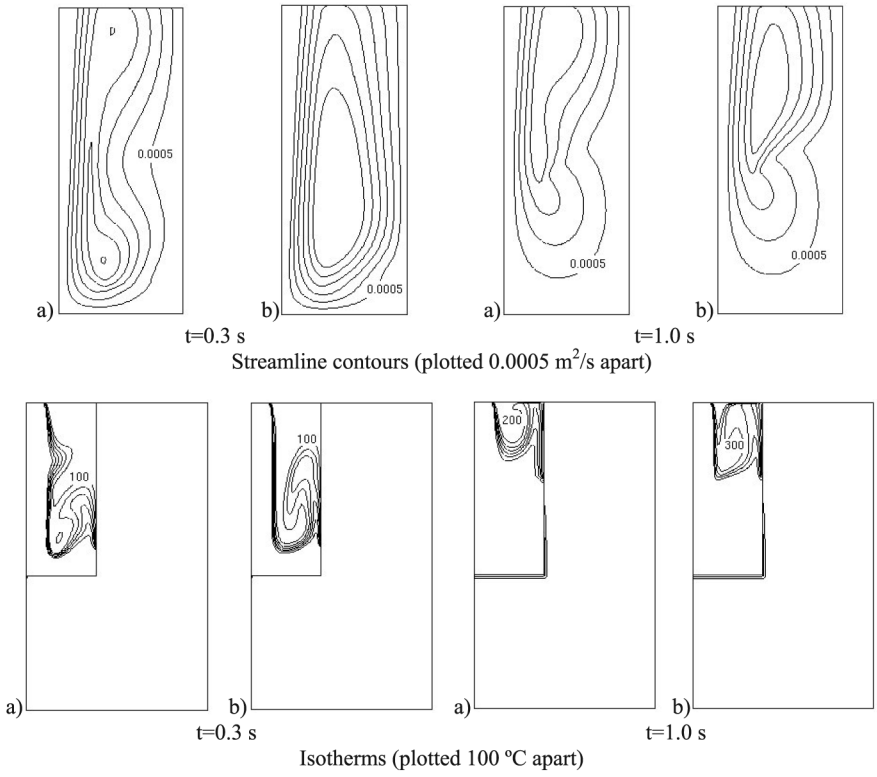

Figure 5.
Aluminum alloy solidification in a sand mould. Streamlines (part, in m^2/s) and isotherms (part and mould, in °C) contours during filling for cases: (a) without buoyancy effects and (b) with buoyancy effects

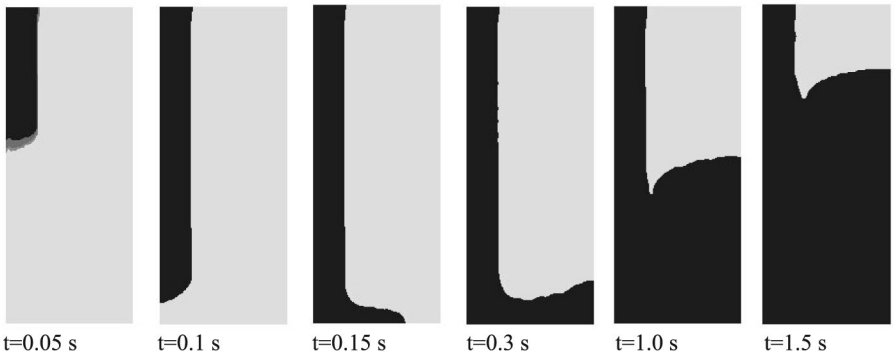

Figure 6.
Aluminum alloy solidification test in a sand mould. Phase-change function evolution during filling (including buoyancy effects)

times of the analysis due to the thermal shock produced by the difference between the initial temperatures of the metal and air (700 and 20°C, respectively).

Fluid motion and temperature evolutions that take place before the beginning of solidification are described in Figure 7 where natural convection evolves against the inertial effects derived from the fluid motion after the

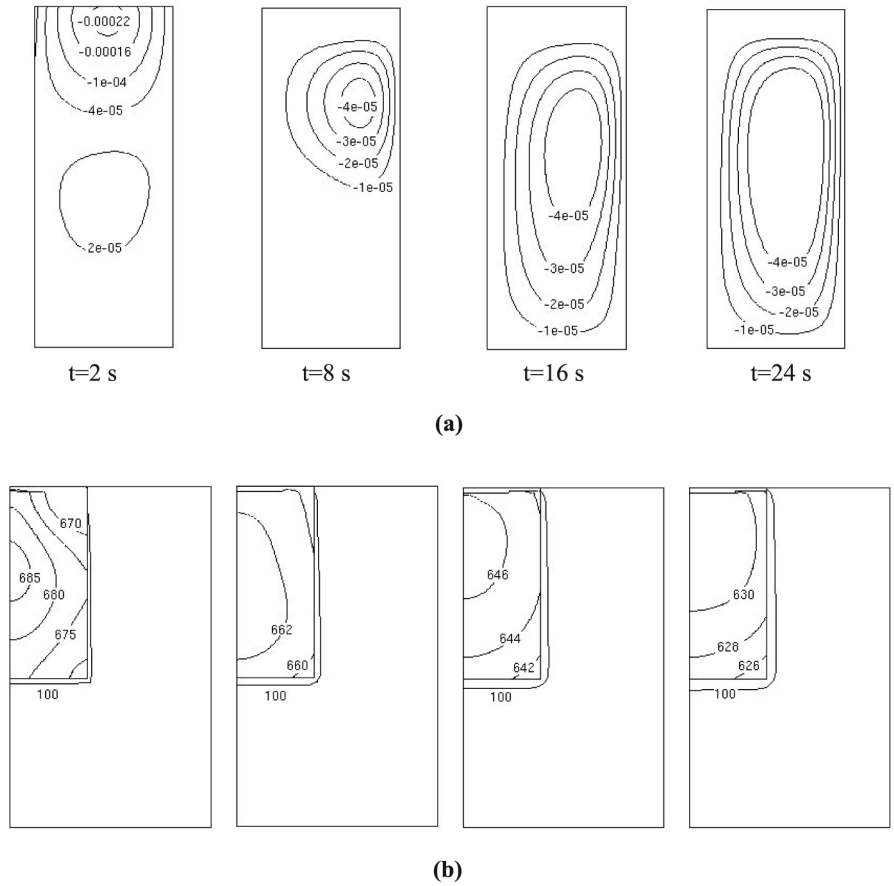

Figure 7.
Aluminum alloy solidification test in a sand mould. (a) Streamlines (part, in m^2/s) and (b) isotherms (part and mould, in °C) before solidification

filling. In spite of the short filling time, the temperature distribution at the end of the pouring process is not uniform. In particular, at $t = 2\,s$ the temperature differs at least in 15°C from the initial pouring temperature. It is important to note that this effect is neglected in simulations that do not include a thermally coupled filling analysis which assume, typically, a uniform temperature distribution once the cavity is completely filled. The temperature evolves practically uniform during the subsequent times of this analysis. Figure 8 shows streamlines, isotherms and liquid fractions during the phase-change process.

Different studies have been performed to illustrate the effect of constant heat transfer coefficients using a purely thermal analysis (T) and the effect of a gap-dependent heat transfer coefficient. In the latter case, a thermomechanical (TM) formulation is compulsorily needed. This analysis assumes an instantaneous filling with a uniform initial casting temperature of 700°C.

Experimental and computed temperature evolutions at the midheight of the specimen at thermocouples 1 and 2 are plotted in Figure 9(a). The value of the heat transfer coefficient can be handled (between a feasible range) to reasonably capture the primary and eutectic transformations as well as the total solidification time. As expected, the temperature evolution is strongly affected by the heat transfer conditions at the casting-mould interface. The curve corresponding to the TM prediction approximately adjusts the measured solidification time presenting, in particular, a similar slope to that of the experimental data in the cooling phase. Additionally, a FTM analysis also considering instantaneous filling with $T_0 = 700$°C and $h = h(g_n)$ has been performed to check the influence of the buoyancy effects on the thermal response. In this case, it should be mentioned that very similar results to those computed with the TM model have been obtained (results not shown). Hence, this fact demonstrates that the natural convection is not relevant in this problem due to the uniformity in the temperature distribution in the liquid phase caused by a low cooling rate mainly obtained as a consequence of the low-thermal diffusivity of the sand.

The effect of the temperature distribution at the end of the filling stage on the thermal response is assessed by means of a FTM analysis including filling in comparison with a TM simulation assuming instantaneous filling with $T_0 = 700$°C. The corresponding numerical predictions are presented in Figure 9(b). As can be noticed, different final solidification are given by these analyses where, in particular, the FTM results satisfactorily match the experimental data in the part.

Finally, the radial displacement history at the midheight casting-mould interface computed in the former FTM analysis is shown in Figure 10. As can be seen, the gap formation starts once the solid fraction reaches a value of approximately 0.30 in the regions near the casting-mould interface.

4.1.2 Casting in a steel mould. The aluminum casting in a steel mould is also analyzed to study the effects of higher cooling rates promoted by a large thermal diffusivity of the mould. This fact is expected to produce large temperature gradients in the part leading, therefore, to a non-negligible effect of the buoyancy forces on the thermal behavior. For simplicity, instantaneous filling with $T_0 = 700$°C is assumed. In this case, an initial mould preheat of 300°C is considered. Figure 11 shows the temperature evolutions at thermocouples 1 and 2 using the TM and FTM formulations. In sharp contrast to the results shown for the sand mould case, large temperature differences are now obtained between both approaches denoting the strong influence of natural convection on the temperature pattern when a steel mould is used. Moreover, the TM simulation not only delays the final solidification time but also modifies the solidification path for both the primary and eutectic transformations. The results obtained with the FTM approach are close to the experimental ones.

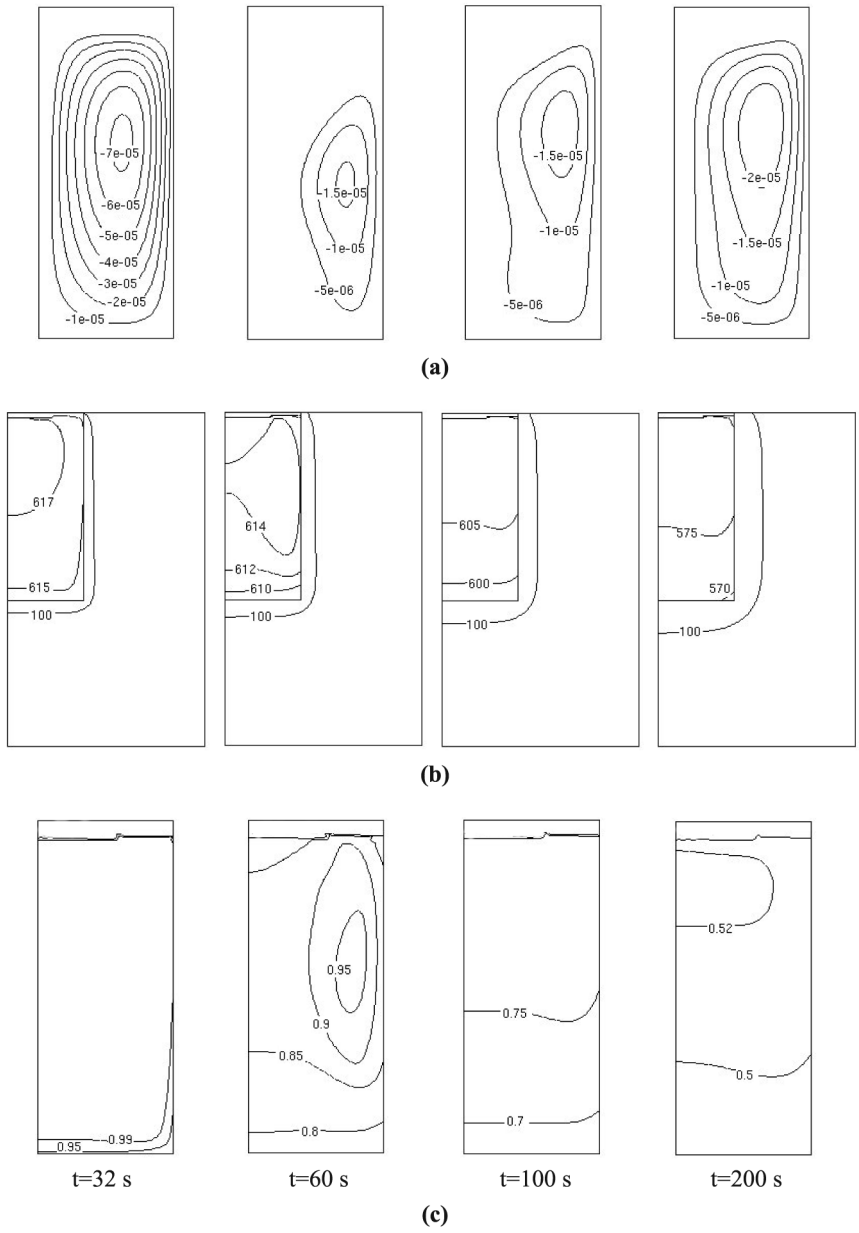

Figure 8.
Aluminum alloy solidification test in a sand mould.
(a) Streamlines (part, in m^2/s), (b) isotherms (part and mould, in °C) and (c) phase-change function (part) during solidification

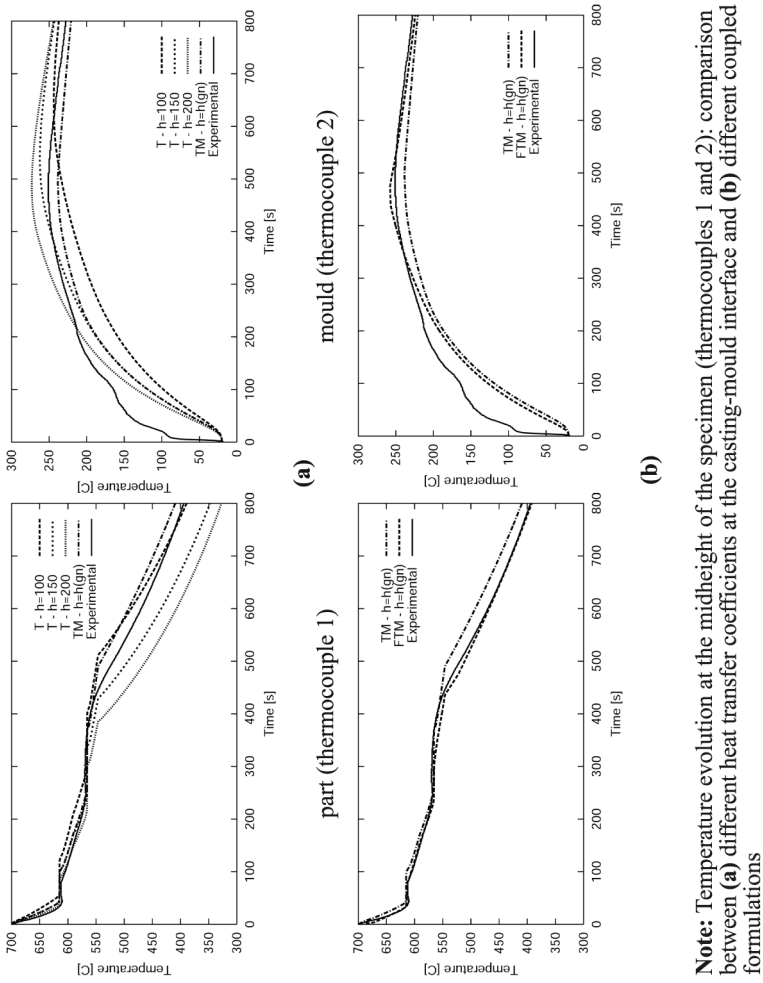

Note: Temperature evolution at the midheight of the specimen (thermocouples 1 and 2): comparison between **(a)** different heat transfer coefficients at the casting-mould interface and **(b)** different coupled formulations

Figure 9.
Aluminum alloy solidification test in a sand mould

4.2 Light alloy solidification in a permanent composite mould

The objective of this analysis is to assess the performance of the present formulation applied to a commercial aluminum alloy Al-7Si-0.3Mg gravity cast in a permanent composite mould of H13 steel and beryllium copper with a bottom insulation. The casting geometry was a stepped vertical cylindrical block as shown in Figure 12. The materials involved in the mould were selected on the basis of their thermal properties and assembled and operated in such a way so as to promote directional solidification of the casting. A detailed description of the geometry, experiment setup, material properties and finite element discretization can be found in the work of Celentano *et al.* (1999) where an exhaustive analysis of this problem has been performed using a

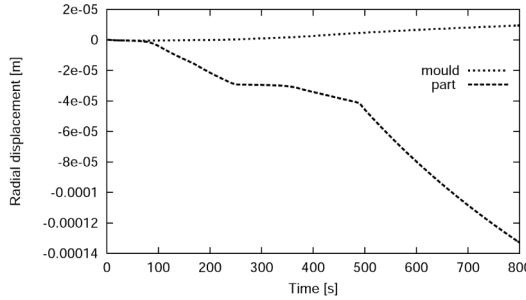

Figure 10.
Aluminum alloy solidification test in a sand mould. Radial displacement evolution at the midheight casting-mould interface

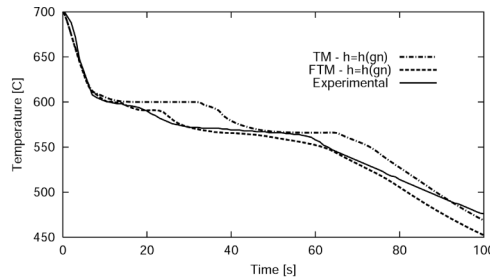

(a)

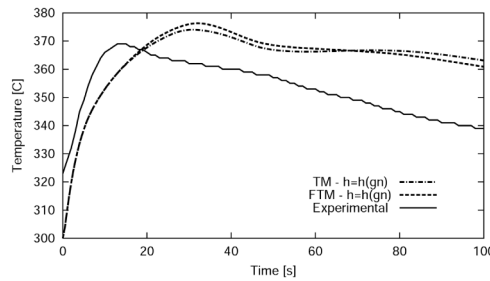

(b)

Figure 11.
Aluminum alloy solidification test in a steel mould. Temperature evolution at (a) thermocouple 1 and (b) thermocouple 2

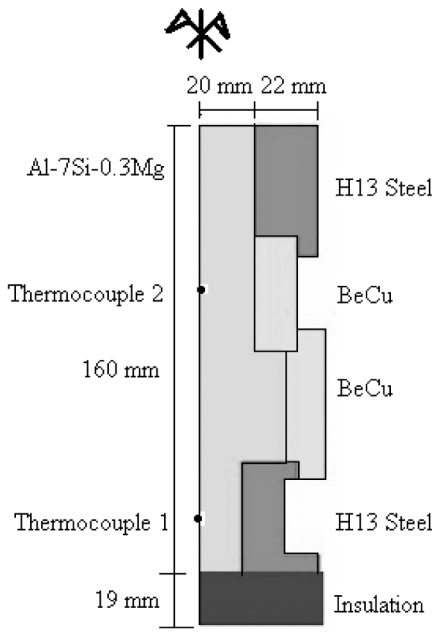

Figure 12.
Light alloy solidification in a permanent composite mould: problem layout

thermomechanical formulation (TM). The referred work also provides experimental validation for the advectionless thermomechanical model. Additionally, the gap-dependent casting-mould heat transfer coefficients were obtained via an inverse purely conductive thermal analysis involving the temperature evolutions and gap histories measured in the laboratory. Owing to this fact, the mentioned heat transfer coefficients directly incorporate other heat transfer mechanisms derived from different physical aspects of the process such as natural convection and fluid motion during filling. In the present work, the influence of natural convection in the solidification patterns is particularly evaluated by comparing different temperature evolutions in the advection (FTM) and advectionless (TM) approaches. To this end, both models are applied in the analysis of this problem using the heat transfer coefficients reported by Celentano (2002) assuming, for simplicity, instantaneous filling (the casting and mould initial temperatures correspond to the forced cooling case presented in such reference).

The temperature evolution obtained at thermocouples 1 and 2 are presented in Figure 13(a) where the natural convection effect is apparent in the FTM simulation giving foreseeable larger cooling rates than those obtained with the TM solution. Nevertheless, as the heat transfer coefficients used in the computations are physically affected by natural convection, an additional study of the numerical behavior of the FTM formulation has been performed using a reduced value of such coefficients to obtain numerical results that properly

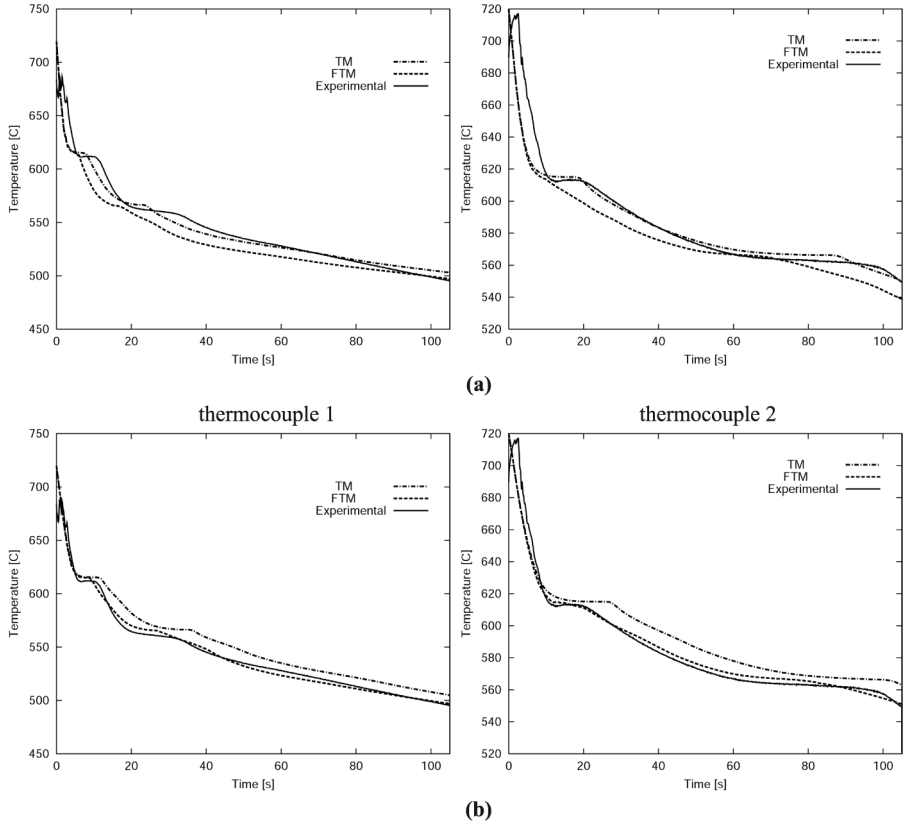

Figure 13.
Light alloy solidification in a permanent composite mould

Note: Temperature evolution at thermocouples 1 and 2 computed with (a) an experimentally-based gap-dependent heat transfer coefficient including natural convection effects in its definition and (b) a modified gap-dependent heat transfer coefficient without natural convection effects in its definition

match the experimental ones. Figure 13(b) shows the temperature evolution computed with a 50 percent reduction of the heat transfer coefficients applying both numerical approaches (TM and FTM). Once again, the effect of considering the fluid dynamics during the process is apparent. It is important to remark that the results obtained with a TM formulation including heat transfer coefficients which incorporate fluid motion effects (as in the case when they are computed from experimental data using inverse analysis that only considers conduction as the unique heat transfer mechanism) are close to those computed with a FTM formulation using a reduced value of such coefficients. Therefore, this comparison allows a proper estimation of the contribution of the advective effects on the heat transfer conditions at the casting-mould interface. These results also show that the fluid motion plays an important role in the

solidification process of this kind of problems and, moreover, an advectionless heat transfer coefficient determination will be relevant to extend its application using FTM simulations to other geometrical configurations involving the same materials.

5. Concluding remarks

A coupled multi-physics model for the integrated analysis of casting processes has been presented and applied to two solidification tests. The advective effects have been found to modify the thermomechanical material response. The filling affects the initial conditions of the solidification stage while the fluid motion caused by natural convection modifies the thermal response during the phase-change process and, specifically, the prediction of the final solidification time. A comparison with available experimental data has also been done. However, future research is still needed to more properly describe and experimentally validate the complex phenomena that take place during solidification processes such as microstructure evolution, shrinkage formation and macro-microsegregation.

References

Bellet, M., Decultieux, F., Ménaï, M., Bai, F., Levaillant, C., Chenot, J., Schmidt, P. and Svensson, I. (1996), "Thermomechanics of the cooling stage in casting processes: three-dimensional finite element analysis and experimental validation", *Metallurgical and Materials Transactions B*, Vol. 27B, p. 81.

Celentano, D. (2001), "A large strain thermoviscoplastic formulation for the solidification of S.G. cast iron in a green sand mould", *International Journal of Plasticity*, Vol. 17, pp. 1623-58.

Celentano, D. (2002), "A thermomechanical model with microstructure evolution for aluminium alloys casting processes", *International Journal of Plasticity*, Vol. 18, pp. 1291-335.

Celentano, D. and Cruchaga, M. (1999), "A thermally coupled flow formulation with microstructure evolution for hypoeutectic cast iron solidification", *Metallurgical and Materials Transactions B*, Vol. 30B, pp. 731-44.

Celentano, D., Gunasegaram, D. and Nguyen, T. (1999), "A thermomechanical model for the analysis of light alloy solidification in a composite mould", *International Journal of Solids and Structures*, Vol. 36, pp. 2341-78.

Chow, P., Bailey, C., Cross, M. and Pericleous, K. (1995), "Integrated numerical modelling of the complete casting process", *Modelling of Casting, Welding and Advanced Solidification Processes VII*, The Minerals, Metals and Materials Society, pp. 213-21.

Cruchaga, M. and Celentano, D. (2000), "A finite element thermally coupled flow formulation for phase-change problems", *International Journal for Numerical Methods in Fluids*, Vol. 34, pp. 279-305.

Cruchaga, M. and Celentano, D. (2001), "A fixed-mesh finite element thermally coupled flow formulation for the analysis of melting processes", *International Journal for Numerical Methods in Engineering*, Vol. 51, pp. 1231-58.

Cruchaga, M. and Celentano, D. (2002), "Numerical analysis of thermally coupled flow problems with interfaces and phase-change effects", *International Journal of Computational Fluid Dynamics*, Vol. 16, pp. 247-62.

Cruchaga, M., Celentano, D. and Tezduyar, T. (2002a), "Computation of mould filling processes with a moving Lagrangian interface technique", *Communications in Numerical Methods in Engineering*, Vol. 18, pp. 483-93.

Cruchaga, M., Celentano, D. and Tezduyar, T. (2002b), "Computation of moving interface problems with the edge-traked interface locator technique", in Mang, H.A., Rammerstorfer, F.G. and Eberhardsteiner, J. (Eds), *Proceedings of the V World Congress on Computational Mechanics*, Vienna, Austria, CD-ROM.

Felicelli, S.D., Heinrich, J.C. and Poirier, D.R. (1998), "Three-dimensional simulations of freckles in binary alloys", *Journal of Crystal Growth*, Vol. 191, pp. 879-88.

Gu, J.P. and Beckermann, C. (1999), "Simulation of convection and macrosegregation in a large steel ingot", *Metallurgical and Materials Transactions A*, Vol. 30a, pp. 1357-66.

Guthrie, R.I.L. and Tavares, R.P. (1998), "Mathematical and physical modelling of steel flow and solidification in twin-roll/horizontal belt thin-strip casting machines", *Applied Mathematical Modelling*, Vol. 22, pp. 851-72.

Heinrich, J.C. and McBride, E. (2000), "Calculation of pressure in a mushy zone", *International Journal for Numerical Methods in Engineering*, Vol. 47, pp. 735-47.

Lewis, R. and Ravindran, K. (2000), "Finite element simulation of metal casting", *International Journal for Numerical Methods in Engineering*, Vol. 47, pp. 29-59.

Naterer, G.F. (1997), "Simultaneous pressure-velocity coupling in the two-phase zone solidification shrinkage in an open cavity", *Modelling Simul. Mater. Sci. Eng.*, Vol. 5, pp. 595-613.

Nigro, N., Huespe, A. and Fachinotti, V. (2000), "Phasewise numerical integration of finite element method applied to solidification processes", *International Journal of Heat and Mass Transfer*, Vol. 43, pp. 1053-66.

Rappaz, M., Drezet, J.M. and Gremaud, M. (1999), "A new hot-tearing criterion", *Metallurgical and Materials Transactions A*, Vol. 30A, pp. 449-55.

Sobh, N., Huang, J., Haber, R.B., Tortorelli, D.A. and Hyland, R.W. Jr. (2000), "A discontinuous Galerkin model for precipitate nucleation and growth in aluminium alloy quench processes", *International Journal for Numerical Methods in Engineering*, Vol. 47, pp. 749-67.

Tezduyar, T. (2001), "Finite element methods for flow problems with moving boundaries and interfaces", *Archives of Computational Methods in Engineering*, Vol. 8, pp. 83-130.

Voller, V.R. (2000), "A model of microsegregation during binary alloy solidification", *International Journal of Heat and Mass Transfer*, Vol. 43, pp. 2047-52.

Voller, V.R. and Beckermann, C. (1999), "A unified model of microsegregation and coarsening", *Metallurgical and Materials Transactions A*, Vol. 30A, pp. 2183-9.

Vreeman, C.J. and Incropera, F.P. (2000), "The effect of free-floating dendrites and convection on macrosegregation in direct chill cast aluminum alloys. Part II: predictions for Al-Cu and Al-Mg", *International Journal of Heat and Mass Transfer*, Vol. 43, pp. 687-704.

Vreeman, C.J., Krane, M.J.M. and Incropera, F.P. (2000), "The effect of free-floating dendrites and convection on macrosegregation in direct chill cast aluminum alloys. Part I: model development", *International Journal of Heat and Mass Transfer*, Vol. 43, pp. 677-86.

Yun, M., Lokyer, S. and Hunt, J. (2000), "Twin roll casting of aluminium alloy", *Materials Science and Engineering*, Vol. A28, pp. 116-23.